

## Comment on: “Anomalous reflection from a two-layered marine sediment” [J. Acoust. Soc. Am. 155, 1285–1296 (2024)] (L)

Aleksei I. Gudimenko,<sup>1,2</sup> Alyona D. Zakharenko,<sup>1</sup> and Pavel S. Petrov<sup>1,a</sup> 

<sup>1</sup>Geophysical Fluid Dynamics Laboratory, Il'ichev Pacific Oceanological Institute, Vladivostok 690041, Russia

<sup>2</sup>Institute for Applied Mathematics, Vladivostok 690041, Russia

### ABSTRACT:

Buckingham [(2024). J. Acoust. Soc. Am. **155**, 1285–1296] analyzed the dependence of the reflection coefficient on the grazing angle in two-layer marine sediment model. The upper layer in his model consists of a fine-grained material (mud), while seawater and the basement below the mud layer are treated as homogeneous halfspaces. Buckingham's analyses revealed several narrow spikes in this dependence that appeared only in the presence of a sound velocity gradient in the mud layer, a phenomenon he called acoustic glint. His derivation was accomplished for certain specific dependencies of the sound velocity on the depth. Surprisingly, the authors appear to reach the conclusion that for a slightly different vertical sound speed profile in the mud layer the spikes are no longer present in the dependence of the reflection coefficient on the grazing angle. More precisely, the same problem is examined in this letter for the case of an  $n^2$ -linear layer (often called Airy medium). Acoustic glint effect is therefore very sensitive to the exact parametrization of the mud layer. © 2024 Acoustical Society of America.

<https://doi.org/10.1121/10.0028366>

(Received 16 May 2024; revised 11 July 2024; accepted 18 July 2024; published online 4 September 2024)

[Editor: John A. Colosi]

Pages: 1524–1527

### I. INTRODUCTION

Investigation of acoustic reflection from the seabed in a shallow sea is considered a useful tool for reconstruction of the geoacoustic parameters of the bottom (Buckingham, 2024; Holland *et al.*, 2022; Katsnelson *et al.*, 2022;). In particular, the positions of maxima and minima of the reflection coefficient considered as a function of the grazing angle at different sound frequencies can be used for sediment characterization (Buckingham, 2024; Holland *et al.*, 2022). Thus, investigation of this dependence for various parametrizations of the sound speed in the sediment could be of importance for the interpretation of seabed reflection data. An interesting feature of the reflection coefficient  $R$  dependence on the grazing angle  $\theta$  for certain frequencies in the case of a two-layer bottom modes was recently theoretically predicted by Buckingham (2024). The feature manifests as a series of very sharp maxima of the function  $R(\theta)$  called acoustic glint. It can be observed for a seabed model in which a sediment layer with an upward-refracting sound speed gradient overlies another (basement) layer. In particular, this model is considered adequate for simulation of the seabed at the New England Mud Patch (NEMP) (Holland, 2021; Holland *et al.*, 2022).

The acoustic glint phenomenon was discovered by considering an analytical expression for the reflection coefficient for two different parametrizations of the sound speed profile in the mud layer, namely, for a linear dependence of the sound speed on the depth and for an inverse-square

profile. Buckingham analyzed the behaviour of the reflection coefficient by expressing it in terms of special functions (linearly independent solutions for the two considered sound speed profiles in the top layer) and then by recasting it using certain integral formulas for these functions.

Motivated by an exciting result reported in Buckingham (2024), we attempted to reproduce it using what we consider a most natural parametrization of the gradient layer. In this study the top sediment is considered an Airy medium (Brekhovskikh and Lysanov, 2003), where the refractive index is a linear function of depth (sometimes this is also called  $n^2$ -linear medium). The solution in such a layer can be written in terms of well-known Airy functions that are often used to construct uniform asymptotic formulas for solutions of various boundary-value problems, since these functions can be accurately and efficiently computed by any mathematical software.

The result of our calculations was rather surprising, as no acoustic glint is observed for our parametrization of the top sediment layer, despite the fact that the sound-speed profile of the Airy medium is almost visually indistinguishable from the one used by Buckingham. This implies that acoustic glint effect is likely to be very sensitive to exact shape of variations of the sound speed in the top sediment layer.

### II. PROBLEM STATEMENT

Consider the system of coupled wave equations describing sound propagation in a three-layer environment shown in Fig. 1

<sup>a</sup>Email: petrov@poi.dvo.ru

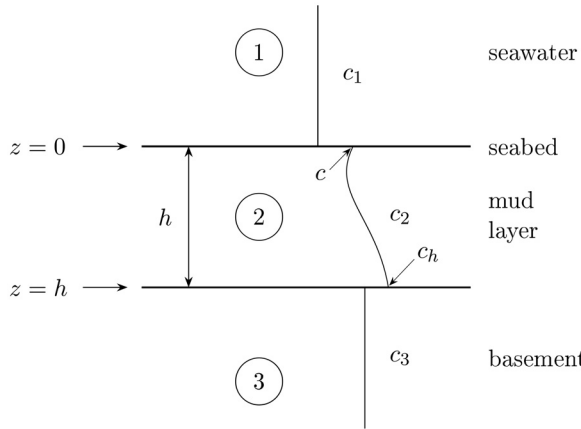


FIG. 1. A shallow-water waveguide consisting of the water column (considered a halfspace unbounded from above) and a two-layer bottom.

$$\begin{aligned}
 -\frac{1}{c_1^2} \frac{\partial^2 u_1}{\partial t^2} + \Delta u_1 &= -q\delta(x)\delta(z - z_0), & z < 0; \\
 -\frac{1}{c_2^2} \frac{\partial^2 u_2}{\partial t^2} + \Delta u_2 &= 0, & 0 < z < h; \\
 -\frac{1}{c_3^2} \frac{\partial^2 u_3}{\partial t^2} + \Delta u_3 &= 0, & z > h,
 \end{aligned} \tag{1}$$

with boundary conditions

$$\begin{aligned}
 u_1(t, x, 0) &= u_2(t, x, 0), \\
 \frac{\partial u_1}{\partial z}(t, x, 0) &= \rho_{12} \frac{\partial u_2}{\partial z}(t, x, 0); \\
 u_2(t, x, h) &= u_3(t, x, h), \\
 \rho_{32} \frac{\partial u_2}{\partial z}(t, x, h) &= \frac{\partial u_3}{\partial z}(t, x, h),
 \end{aligned} \tag{2}$$

where  $\rho_{ij} = \rho_i/\rho_j$ .

Let us apply Fourier transform  $u_j(t, x, z) \rightarrow \hat{u}_j(\omega, k, z)$  to Eqs. (1) and (2),  $j = 1, 2, 3$ , and introduce the notation

$$\kappa_j = \sqrt{k_j^2 - k^2}, \quad k_j = \frac{\omega}{c_j}, \quad j = 1, 2, 3. \tag{3}$$

We obtain the following boundary-value problem in the frequency domain:

$$\hat{u}_j'' + \kappa_j^2 \hat{u}_j = -q\delta(z - z_0)\delta_{j,1}, \quad j = 1, 2, 3; \tag{4}$$

$$\begin{aligned}
 \hat{u}_1(0) &= \hat{u}_2(0), & \hat{u}_1'(0) &= \rho_{12}\hat{u}_2'(0); \\
 \hat{u}_2(h) &= \hat{u}_3(h), & \rho_{32}\hat{u}_2'(h) &= \hat{u}_3'(h),
 \end{aligned} \tag{5}$$

where a prime denotes differentiation with respect to  $z$ . In order to simplify the notation, hereafter we omit the variables  $\omega$  and  $k$  in the functions  $\hat{u}_j, j = 1, 2, 3$ .

### III. FORMULA FOR THE REFLECTION COEFFICIENT

Let us now derive the solution to the BVP for Eq. (4) with the boundary conditions (BCs) Eq. (5). Note that we

closely follow the derivations from Buckingham (2024, 2023) without specifying an exact form of the sound speed profile  $c_2(z)$  in the upper sediment layer and, consequently, expressing the solution within this layer in terms of two (so far unknown) linearly independent functions. As a result, the formulas below cover both cases considered by Buckingham (namely, the linear and the inverse-square sound speed profiles) as well as the case of the Airy medium studied in Sec. IV.

The solutions of the first and the third equations of the system (4) can be written in the form

$$\hat{u}_1 = \left[ \frac{\hat{u}_1(0)}{2} + \frac{\hat{u}_1'(0)}{2i\kappa_1} \right] e^{i\kappa_1 z} + \frac{q e^{-i|z-z_0|\kappa_1}}{2i\kappa_1}, \tag{6}$$

$$\hat{u}_3 = \hat{u}_3(h) e^{-i(z-h)\kappa_3}. \tag{7}$$

Let us write the solution of the second equation as

$$\hat{u}_2 = a(\omega, k)f(z) + b(\omega, k)g(z), \tag{8}$$

where  $f$  and  $g$  are two arbitrary linearly independent solutions of this equation. Imposing BCs (5), we obtain the following equalities:

$$\begin{aligned}
 \frac{\hat{u}_1(0)}{2} + \frac{\hat{u}_1'(0)}{2i\kappa_1} + \frac{q e^{i z_0 \kappa_1}}{2i\kappa_1} &= af(0) + bg(0), \\
 i\kappa_1 \left[ \frac{\hat{u}_1(0)}{2} + \frac{\hat{u}_1'(0)}{2i\kappa_1} \right] - \frac{q e^{i z_0 \kappa_1}}{2} &= \rho_{12} [af'(0) + bg'(0)], \\
 \hat{u}_3(h) &= af(h) + bg(h), \\
 -i\kappa_3 \hat{u}_3(h) &= \rho_{32} [af'(h) + bg'(h)],
 \end{aligned} \tag{9}$$

from which we can find the unknown coefficients in Eqs. (6) and (8).

Eliminating from the latter system of equations (9) the quantities  $\hat{u}_1(0), \hat{u}_1'(0),$  and  $\hat{u}_3(h),$  we arrive at a system of linear equations of the form  $A\chi = \beta,$  where

$$\chi = [a, b]^T, \quad \beta = [q e^{i z_0 \kappa_1}, 0]^T,$$

are column vectors corresponding to the coefficients in the linear combination in Eq. (8) and to the input term (i.e., the point source), respectively, while  $A$  is a matrix

$$A = \begin{bmatrix} i\kappa_1 f(0) - \rho_{12} f'(0) & i\kappa_1 g(0) - \rho_{12} g'(0) \\ i\kappa_3 f(h) + \rho_{32} f'(h) & i\kappa_3 g(h) + \rho_{32} g'(h) \end{bmatrix}.$$

The solution  $\chi$  of this linear system is easily obtained by the Cramer's rule

$$\begin{aligned}
 a &= \frac{i\kappa_3 g(h) + \rho_{32} g'(h)}{\det A} q e^{i z_0 \kappa_1}, \\
 b &= -\frac{i\kappa_3 f(h) + \rho_{32} f'(h)}{\det A} q e^{i z_0 \kappa_1}.
 \end{aligned} \tag{10}$$

Now we introduce the reflection coefficient  $R = R(k)$  via the following relationship:

$$\hat{u}_1 = \frac{q}{2i\alpha_1} (e^{-i|z-z_0|\alpha_1} + R e^{-i|z+z_0|\alpha_1}). \quad (11)$$

From Eqs. (6), (9), (10), and (11) we easily find that

$$R = -\det B(\det A)^{-1}, \quad (12)$$

and  $B$  is the matrix obtained from  $A$  by a substitution  $\alpha_1 \rightarrow -\alpha_1$ . An explicit formula for  $\det A$  is written as

$$\begin{aligned} \det A = & -\alpha_1 \alpha_3 [f(0)g(h) - f(h)g(0)] \\ & - \rho_{12} \rho_{32} [f'(0)g'(h) - f'(h)g'(0)] \\ & + i\alpha_1 \rho_{32} [f(0)g'(h) - f'(h)g(0)] \\ & + i\alpha_3 \rho_{12} [f(h)g'(0) - f'(0)g(h)]. \end{aligned} \quad (13)$$

Similarly, substituting Eq. (10) into the third equation of the system (9), we find the quantity  $\hat{u}_3(h)$ . Its value together with the expressions Eq. (11) and Eqs. (6)–(8) fully determines the solution of the BVP in Eqs. (4) and (5).

Different sound speed profiles in the top sediment layer can all be described by Eq. (12) with particular solutions  $f$  and  $g$  chosen accordingly.

#### IV. THE SOLUTION FOR AN $n^2$ -LINEAR PROFILE IN THE TOP LAYER

Note that we have not specified the sound speed profile in the layer with the gradient until now. In this section we investigate one particular case assuming that this layer in an Airy medium, i.e., that the refractive index squared is a linear function

$$c_2 = \frac{c}{\sqrt{\alpha z + 1}}. \quad (14)$$

Note that hereafter we assume that  $\alpha$  is negative, so that the profile is upward-refracting. Then Airy functions Ai and Bi can be taken as a pair of linearly independent solutions in Eq. (8),

$$f(z) = \text{Ai}[\zeta(z)], \quad g(z) = \text{Bi}[\zeta(z)],$$

where

$$\zeta = -\left(\frac{c^2}{\omega^2 \alpha}\right)^{2/3} \left(\frac{\omega^2}{c^2} - k^2\right).$$

In this case, Eq. (12) allows one to perform the computations both very accurately and efficiently using practically any mathematical software (see supplementary material for an implementation in MATLAB).

Let us set the following values for the media parameters.

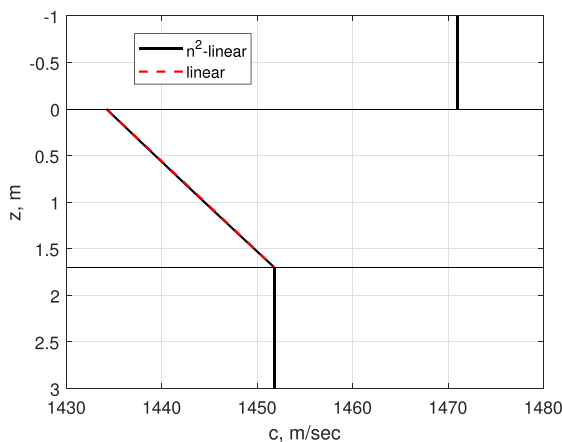
##### Case 1: Slow basement

$$\begin{aligned} c_1 = 1471, \quad c = 1434.21, \quad c_h = 1451.8, \\ c_3 = 1451.8, \quad \alpha = -0.0142, \\ \rho_1 = 1023, \quad \rho_2 = 1600, \quad \rho_3 = 1650, \\ h = 1.7. \end{aligned} \quad (15)$$

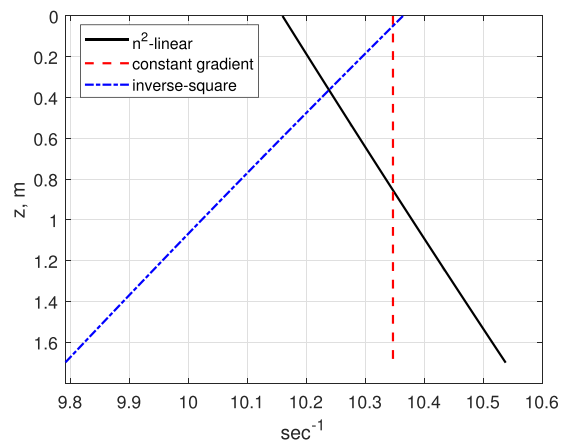
##### Case 2: Fast basement

$$\begin{aligned} c_1 = 1471, \quad c = 1434.21, \quad c_h = 1451.8, \\ c_3 = 1678.7, \quad \alpha = -0.0286, \\ \rho_1 = 1023, \quad \rho_2 = 1600, \quad \rho_3 = 1650, \\ h = 1.7. \end{aligned} \quad (16)$$

For the specified values of the geoacoustic parameters (15), (16) the sound speed profiles in the mud layer are practically linear in  $z$  [see Fig. 2(a)], and therefore nearly indistinguishable from those considered in Buckingham (2024) [see Fig. 2(a), where the profile used here is plotted against the linear in  $z$  profiles from Buckingham (2024)]. The difference between the profiles from Buckingham (2024) and the  $n^2$ -linear profile can be better understood by considering respective sound speed gradients shown in Fig. 2(b).



(a) sound speed



(b) sound speed gradient

FIG. 2. (Color online) Sound speed profiles in the waveguide model with a two-layer seabed: linear dependence of the sound speed on depth in the top sediment layer (dashed line) and a similar  $n^2$ -linear profile (solid line) (a) and gradients of the sound speed in the upper sediment layer for these two cases as well as for the inverse-square profile also considered in Buckingham (2024) (b).

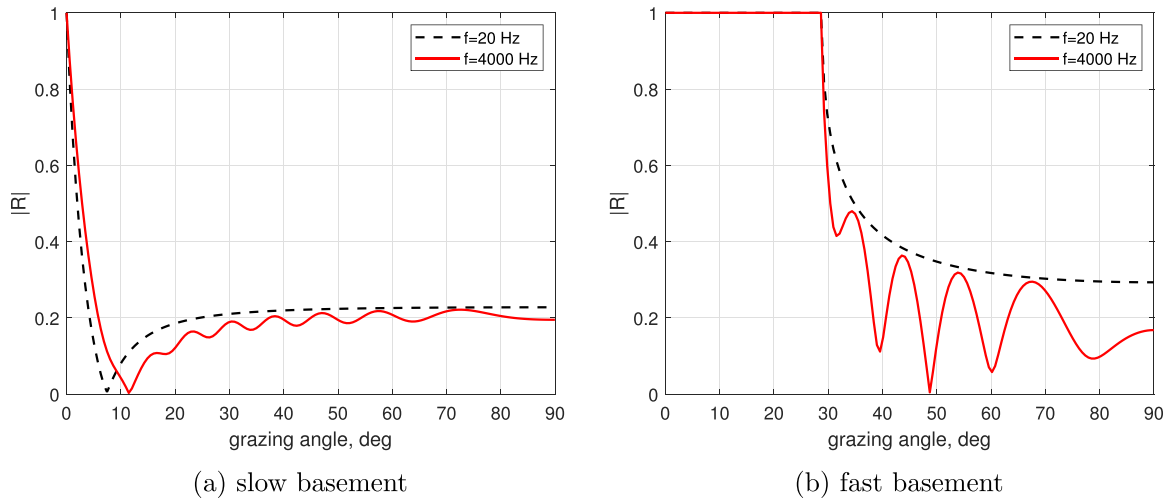


FIG. 3. (Color online) The dependence of the coefficient of reflection from the seabed computed directly by Eq. (12) for the slow basement (a) and fast basement (b) cases. Dashed and solid lines correspond to the frequencies  $f = 20$  and 4000 Hz, respectively.

Let us now set

$$k = \frac{\omega}{c_1} \cos \theta$$

in Eq. (3), i.e., consider the reflection of a plane wave

$$u_1 \sim -e^{-i\omega t} [e^{i(kx + \alpha_1|z - z_0|)} + R e^{i(kx + \alpha_1|z + z_0|)}]$$

with a grazing angle  $\theta$  from a two-layer seabed. In this case we can consider  $R$  a function of  $\theta$  instead of  $k$ .

The behaviour of the modulus of the reflection coefficient  $|R|$  as a function of  $\theta$  is shown in Fig. 3 both for the slow [geoacoustic parameters in Eq. (15)] and the fast [parameters in Eq. (16)] basement case cases [subplots (a) and (b), respectively]. It can be seen that no anomalous reflection spikes are present in these graph, by contrast to the plots in (Buckingham, 2024). Therefore, acoustic glint is not manifest if the top sediment layer is an Airy medium.

## V. CONCLUSION AND DISCUSSION

In this comment we closely followed the derivations in Buckingham (2024) and investigated acoustic reflection from a two-layer sediment. Although the upward-refracting sound speed profile in the upper sediment layer in our case is very close to that in Buckingham (2024), and all other model parameters are identical, we did not observe acoustic glint effect.

Let us emphasize that we do not claim that computations in Buckingham's paper are incorrect. Instead, we would like to highlight the fact that acoustic glint effect can actually be very sensitive to the shape of the sound speed profile in the gradient (top) layer of the seabed. Such effects could be rather difficult to observe in real-world environments. Another possibility is that it is essential whether the function describing sound speed dependence on the depth in the gradient layer is convex (inverse-square case) or concave ( $n^2$ -linear case), i.e., whether the sound speed

derivative with respect to  $z$  is increasing or decreasing with the depth [see Fig. 2(b)].

## SUPPLEMENTARY MATERIAL

See the supplementary material for MATLAB script implementing the computations that are used to produce Fig. 3.

## ACKNOWLEDGMENTS

The work of A.Z. was supported by the Russian Science Foundation, project No. 22-11-00171. The work of P.P. and A.G. at POI is within state assignment program No. 121021700341-2.

## AUTHOR DECLARATIONS

### Conflict of Interest

The authors declare no conflict of interest.

## DATA AVAILABILITY

Data availability is not applicable to this article as no new data were collected or analyzed in this study.

- Brekhovskikh, L., and Lysanov, Y. P. (2003). *Fundamentals of Ocean Acoustics* (Spring-Verlag, Berlin).
- Buckingham, M. J. (2023). "On plane-wave reflection from a two-layer marine sediment: A surficial layer with linear sound speed profile overlying an iso-speed basement," *J. Acoust. Soc. Am.* **153**(1), 446–455.
- Buckingham, M. J. (2024). "Anomalous reflection from a two-layered marine sediment," *J. Acoust. Soc. Am.* **155**(2), 1285–1296.
- Holland, C. W. (2021). "Sound speed gradients in mud," *JASA Express Lett.* **1**(6), 066001.
- Holland, C. W., Smith, C. M., Lowe, Z., and Dorminy, J. (2022). "Seabed observations at the New England Mud Patch: Reflection and scattering measurements and direct geoacoustic information," *IEEE J. Oceanic Eng.* **47**(3), 578–593.
- Katsnelson, B., Uzhansky, E., Lunkov, A., and Ostrovsky, I. (2022). "Characterization of the gassy sediment layer in shallow water using an acoustical method: Lake Kinneret as a case study," *Limnology Ocean. Methods* **20**(9), 581–593.